

## Heterogeneous H-Bonding in a Foldamer Helix

Brian F. Fisher, Li Guo,<sup>†</sup> Brian S. Dolinar, Ilia A. Guzei, and Samuel H. Gellman\*

Department of Chemistry, University of Wisconsin-Madison, Madison, Wisconsin 53706, United States

**S** Supporting Information

**ABSTRACT:** Structural characterization of new  $\alpha/\gamma$ -peptide foldamers containing the cyclically constrained  $\gamma$ -amino acid **I** is described. Crystallographic and 2D NMR analysis shows that  $\gamma$  residue **I** promotes the formation of a 12/10-helical secondary structure in  $\alpha/\gamma$ -peptides. This helix contains two different types of internal H-bond, and the data show that the 12-atom  $\text{C}=\text{O}(i) \rightarrow \text{H}-\text{N}(i+3)$  H-bond is more favorable than the 10-atom  $\text{C}=\text{O}(i) \rightarrow \text{H}-\text{N}(i-1)$  H-bond. Several foldamer helices featuring topologically distinct H-bonds have been discovered, but our findings are the first to show that such H-bonds may differ in their favorability.

Biology relies on proteins and nucleic acids to carry out diverse functions, most of which require the biopolymer to adopt a complex and specific folding pattern. The relationship between sophisticated function and higher-order structure has inspired many groups to seek nonbiological oligomers that favor specific conformations (“foldamers”).<sup>1</sup> Extrapolation from the poly- $\alpha$ -amino acid backbone of proteins has led to the study of  $\beta$ -peptides,  $\gamma$ -peptides, and higher homologues.<sup>2</sup> Secondary structural motifs reminiscent of (but geometrically distinct from) those well-known in proteins, including helices, sheets, and reverse turns, have been characterized for these new backbones, and approaches to tertiary structure have been reported.<sup>3</sup> The folding rules established for  $\beta$ - and  $\gamma$ -peptides have enabled the development of specific examples that display biomimetic function.<sup>4</sup>

Expansion beyond the biopolymer prototypes allows deviation from particular structural parameters associated with proteins and nucleic acids. The backbones of these biopolymers, for example, are homogeneous in that each subunit is drawn from a single chemical class (e.g.,  $\alpha$ -amino acids), but heterogeneous backbones are readily accessed among synthetic oligomers.<sup>5</sup> A variety of discrete secondary structures have been identified among peptidic foldamers with mixed backbones, including combinations of  $\alpha + \beta$  residues or  $\alpha + \gamma$  residues. For some applications, such as functional mimicry of a natural  $\alpha$ -helix, heterogeneous backbones containing both  $\alpha$  and  $\beta$  residues have proven to be superior to the homogeneous  $\beta$  residue backbone.<sup>6</sup>

Within the regular helices found in proteins, each type of internal non-covalent contact is topologically equivalent across all of the subunits involved. In an  $\alpha$ -helix, for example, all of the  $\text{C}=\text{O}(i) \rightarrow \text{H}-\text{N}(i+4)$  H-bonds should be comparable to one another, excluding terminal effects, since the  $\text{C}=\text{O}$  and  $\text{H}-\text{N}$  groups are all similar. In contrast, different types of internal H-bonds occur within many of the helices that have been documented among peptidic foldamers with unnatural back-

bones. Such differences are inherent for helices formed by heterogeneous backbones because of subunit diversity. Thus, for example, an  $\alpha/\beta$ -peptide contains H-bond-accepting groups ( $\text{C}=\text{O}$ ) and -donating groups ( $\text{N}-\text{H}$ ) from both  $\alpha$  and  $\beta$  residues. Different types of H-bonds are found also in foldameric helices in which H-bond directionality alternates along the backbone, whether the backbone is homogeneous (as in the  $\beta$ -peptide 10/12-helix<sup>7</sup> and 18/20-helix<sup>8</sup>) or heterogeneous (as in the  $\alpha/\beta$ -peptide 11/9-helix<sup>9</sup> and 18/16-helix<sup>10</sup>). These systems raise a fundamental question: are the different types of intrahelical H-bonds comparably favorable? Here we describe a new type of  $\alpha/\gamma$ -peptide foldamer and provide the first evidence that distinct types of H-bonds formed within a regular secondary structure can differ in terms of favorability.

The new foldamers contain ring-constrained  $\gamma$  residues of type **I** (Figure 1). Either enantiomer of the necessary  $\gamma$ -amino acid

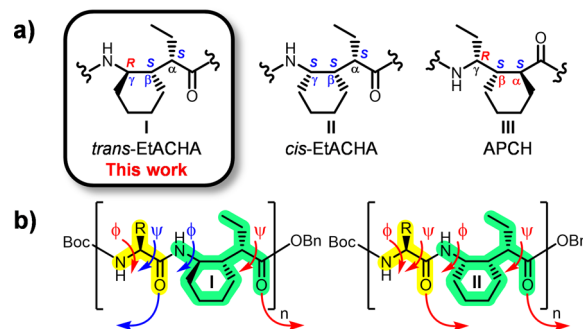


**Figure 1.** (a) Comparison of cyclic  $\gamma$ -amino acids studied by our group. (b) Inversion of the  $\text{C}_\gamma$  stereocenter of **II**, forming **I**, is predicted to invert the adjacent amide H-bond directionality in the full-length H-bonded foldamer.

building block can be efficiently prepared.<sup>11</sup> Previous characterization of oligomers containing the stereoisomeric  $\gamma$  residue of type **II** established that this subunit, alone<sup>12</sup> or in alternation with  $\alpha$  or  $\beta$  residues,<sup>11,13</sup> favors helices defined by  $\text{C}=\text{O}(i) \rightarrow \text{H}-\text{N}(i+3)$  H-bonds. The present studies of  $\alpha/\gamma$ -peptides containing **I** were intended to test the generality of the “stereochemical patterning” hypothesis of Martinek, Fülöp, and co-workers,<sup>14</sup> who proposed a correlation between H-bond directionality within foldamer helices and the signs of the torsion angles about the bonds that flank amide linkages ( $\psi, \phi$  pairs from adjacent residues). If these torsion angles are all of the same sign, then all of the intrahelical H-bonds should be oriented in the same direction (as observed, for example in the  $\alpha$ -helix). If the torsion

Received: March 31, 2015

Published: May 14, 2015

angles alternate between neighboring amides (i.e., if amides that have positive flanking torsion angles are adjacent to amides that have negative flanking torsion angles and vice versa), then intrahelical H-bonds should alternate in directionality relative to the helix axis.

The Martinek–Fülöp hypothesis led us to predict that altering only the stereocenter adjacent to the  $\phi$  torsion angle in  $\gamma$  residues (i.e., **II**  $\rightarrow$  **I**) would cause a wholesale change in helix geometry in  $\alpha/\gamma$ -peptides from a conformation with unidirectional H-bonds to a conformation with bidirectional H-bonds. This prediction relied on the fact that  $\alpha$  residues can readily adopt conformations in which the backbone torsion angles  $\phi$  and  $\psi$  have the same sign ( $\alpha$ -helix) or different signs ( $\beta$ -sheet). To test this prediction,  $\gamma$  residues of type **I** with absolute configuration of (*S,S,R*) at the ( $\alpha,\beta,\gamma$ ) carbons had to be paired with *L*- $\alpha$ -amino acid residues and (*R,R,S*)-**I** with *D*- $\alpha$  residues.

Our initial efforts were aimed at crystallographic characterization of the new  $\alpha/\gamma$ (**I**)-peptides. Seven structures were obtained<sup>15</sup> for oligomers containing four to six residues, three by racemic crystallization.<sup>16</sup> The structures of tetramers **1a–c**, collectively, were not wholly consistent with our expectations. All three formed a 12-atom H-bond between the N-terminal Boc C=O and N–H of the  $\alpha$  residue closest to the C-terminus (Figure 2). This C=O(*i*)  $\rightarrow$  H–N(*i*+3) interaction is

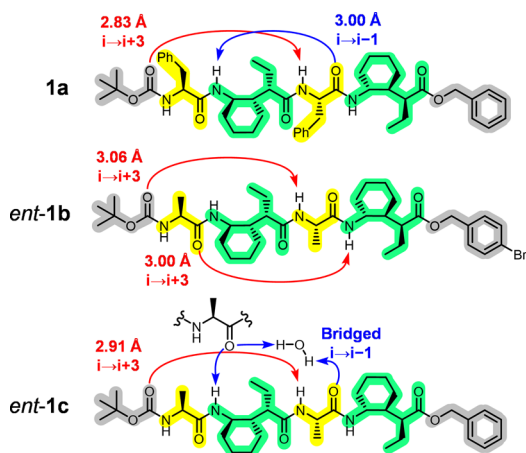


**Figure 2.** Structures of tetramers **1a–c** depicting H-bonds observed in the crystal structures. Enantiomers of **1b** and **1c** are shown.  $\alpha$  residues are shaded in yellow,  $\gamma$  residues in green, and protecting groups in gray. 12-Atom H-bonds are shown in red and 10-atom H-bonds in blue. The geometric criteria used for all of the H-bond assignments are N $\cdots$ O distance < 4.0 Å and N–H $\cdots$ O angle > 130°.

characteristic of both the 12/10-helix we expected and the 12-helix previously documented for  $\alpha/\gamma$ -peptides containing  $\gamma$  residue **II**. Only *rac*-**1a** ( $\alpha$  residues = Phe), however, displayed the 10-atom C=O(*i*)  $\rightarrow$  H–N(*i*–1) H-bond characteristic of the 12/10-helix. In this structure, the 10-atom H-bond was significantly longer than the 12-atom H-bond (N $\cdots$ O = 3.00 vs 2.83 Å). For **1b** ( $\alpha$  residues = Ala), a second 12-atom H-bond formed, i.e., this  $\alpha/\gamma$ -peptide adopted a 12-helix rather than a 12/10-helix.  $\alpha/\gamma$ -Peptide **1c** ( $\alpha$  residues = Ala) displayed an interesting variation on the 10-atom H-bond: the carbonyl of Ala-3 was linked to N–H(*i*–1) via an intermolecular H-bond chain that included a water molecule along with the N-terminal Ala carbonyl of its lattice neighbor.<sup>17</sup>

Longer  $\alpha/\gamma$ -peptides containing  $\gamma$  residue **I** manifested a stronger preference for the 12/10-helix in the solid state, but the

crystal structures offered hints that the 12-atom H-bonds are more favorable than the 10-atom H-bonds. Pentamer **2a** ( $\alpha$  residues = Val) displayed a 12/10-helical conformation in which the maximum number of amide-to-amide H-bonds was formed, two in 12-atom rings and one in a 10-atom ring (Figure 3). All of

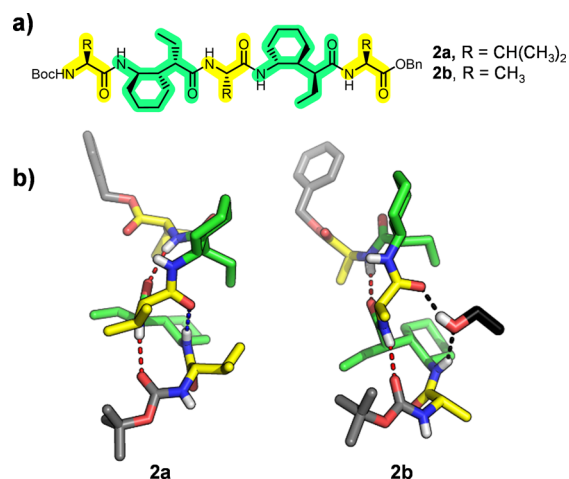


**Figure 3.** (a) Structures of pentamers **2a** and **2b**. (b) Crystal structures of pentamers **2a** and **2b**. Other colors as in Figure 2.

the H-bonded N $\cdots$ O distances in this structure were relatively long (>3.00 Å). The two structurally very similar symmetry-independent conformers of pentamer **2b**<sup>17</sup> ( $\alpha$  residues = Ala) adopted a 12/10-helix-like conformation in the crystal, but an ethanol molecule was found to be interpolated between the C=O and H–N groups that would have formed the 10-atom intrahelical H-bond (Figure 3b). The two 12-atom H-bonds in this structure featured significantly shorter N $\cdots$ O distances than were found in the crystal structure of **2a**.<sup>17</sup>

Hexamer *rac*-**3** ( $\alpha$  residues = Phe) provided two crystal forms under slightly different solvent conditions (Figure 4). One crystal contained a 12/10-helix that seemed to unravel toward the C-terminus; this structure contained two short 12-atom H-bonds (2.85/2.86 Å) and a longer 10-atom H-bond (3.02 Å). A second

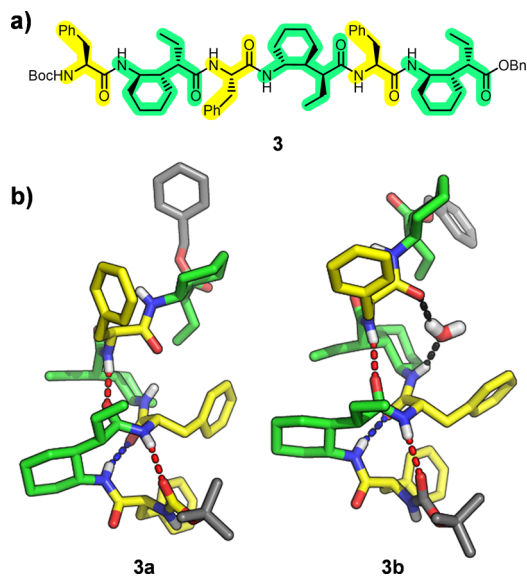


**Figure 4.** (a) Structure of hexamer **3**. (b) Crystal structures **3a** and **3b**. The inserted H<sub>2</sub>O molecule of **3b** is also shown. Colors as in Figure 2.

amide–amide 10-atom H-bond would be possible toward the C-terminus, but in this case the poor geometric parameters ( $N\cdots O$  distance of 4.09 Å and  $N-H\cdots O$  angle of  $135^\circ$ ) suggest that this interaction, if present, is substantially weaker than all of the other H-bonds described here.<sup>18</sup> The other crystalline form of *rac-3* revealed a 12/10-helix-like conformation in which a water molecule was interpolated between the  $C=O$  and  $H-N$  groups that would have formed the C-terminal 10-atom H-bond. The set of seven crystal structures collectively suggests that the new  $\alpha/\gamma$ -peptide backbone has a propensity for 12/10-helix-like conformations but that H-bonding may be more favorable in the 12-atom rings than in the 10-atom rings.

To gain insight into the folding propensity of  $\alpha/\gamma(I)$ -peptides in solution, we employed 2D NMR (COSY, TOCSY, and ROESY) to evaluate the conformations in  $CDCl_3$  of five oligomers containing from five to nine residues. Evidence for 12/10-helical folding was obtained in each case in the form of inter-residue nuclear Overhauser effects (NOEs) between protons separated by 7 to 12 covalent bonds. Here we focus on nonamer **4**. Three nonsequential backbone proton NOE patterns previously reported to be consistent with 12/10-helical secondary structure<sup>19</sup> were observed along most or all of **4** (Figure 5). In addition, we observed a set of strong  $i, i+2$  NOEs

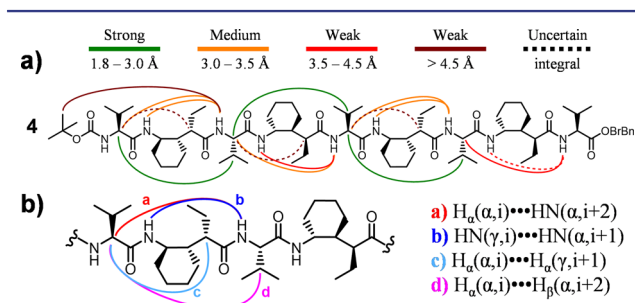


**Figure 5.** (a) Nonsequential ROESY cross-peaks observed in nonamer **4** in  $CDCl_3$ . Uncertain integrals could not be reliably software-integrated. (b) 12/10-Helical cross-peak patterns observed in **4**.

from  $C_\alpha H$  of each Val residue to  $C_\beta H$  of the next Val residue, which is consistent with the 12/10-helical conformation. NMR-restrained simulated annealing calculations were carried out for each of the five oligomers with the Crystallography and NMR System (CNS) software suite (Figure 6). A total of 24 NOE-derived distance restraints from **4** were used to generate an ensemble of 10 lowest-energy structures. The N-terminal four-residue segment in the average generated from these 10 structures overlays well with the crystal structure of pentamer **2a**.

We used H/D exchange (HDX) measurements to test the hypothesis that 12/10-helices formed by the new  $\alpha/\gamma(I)$ -peptide backbone contain H-bond types with different intrinsic favorabilities. These studies focused on the octamer Boc-([Phe] $[\gamma(I)]_4$ -OBn (**5**), for which 2D NMR data provided evidence of 12/10-helical folding in  $CDCl_3$ .<sup>17</sup> Amino acid residue identity exerts a large influence on HDX;<sup>20</sup> therefore, the results for octamer **5**, expressed as half-life ( $t_{1/2}$ ) for disappearance of amide  $^1H$  NMR resonances after dissolution in 95:5  $CDCl_3/CD_3OD$ , were normalized to the results for model dipeptide **6**. Specifically, the  $t_{1/2}$  value for each  $\alpha$  residue NH in **5** was divided by  $t_{1/2}$  for the  $\alpha$  residue NH in **6**, and the  $t_{1/2}$  value for each  $\gamma$  residue in **5** was divided by  $t_{1/2}$  for the  $\gamma$  residue in **6**. This normalization should highlight the impact of folding on HDX at each site within the octamer.

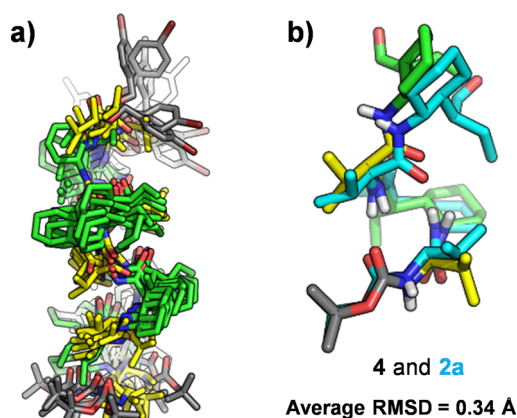


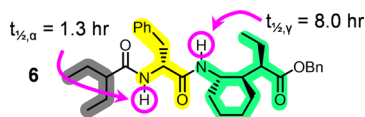
**Figure 6.** (a) NMR ensemble generated by CNS using distance restraints from ROESY data for nonamer **4** in  $CDCl_3$ . The 10 lowest-energy structures were collected from 1000 trial structures. (b) Backbone alignment of the first four residues of the minimized average of the 10 lowest-energy NMR structures with pentamer crystal structure **2a**.

The normalized  $t_{1/2}$  values (Table 1) are generally largest toward the center of **5**, which is consistent with the hypothesis that this  $\alpha/\gamma$ -peptide adopts a helical conformation featuring internal H-bonds of alternating directionality. The  $\alpha$  residue NH resonances show larger normalized  $t_{1/2}$  values than do the  $\gamma$  residue NH resonances. This trend is consistent with the hypothesis that the H-bonds formed by the  $\alpha$  residue NH groups (12-atom rings) are more favorable than the H-bonds formed by the  $\gamma$  residue NH groups (10-atom rings). Further support for the proposed distinction between 12- and 10-atom internal H-bonds was provided by experiments in which small aliquots of dimethyl sulfoxide (DMSO) were added to a  $CDCl_3$  solution of octamer **5** (“DMSO titrations”).<sup>17</sup>

The crystallographic and NMR data reported here show that  $\alpha/\gamma$ -peptide secondary structure can be engineered on the basis of the stereochemical patterning hypothesis of Martinek, Fülöp, and co-workers. Altering just one configuration in the dipeptide repeating unit of the backbone by replacing  $\gamma(II)$  residues with  $\gamma(I)$  residues leads to a change in conformational preference from a helix with unidirectional H-bonds to a helix in which the H-bond direction alternates. The ability to alter the helix type by switching a single configuration within the  $\gamma$  residues represents a significant accomplishment in foldamer design.

Exploration of the new  $\alpha/\gamma(I)$  backbone led to the unexpected discovery that the 12/10-helix formed by these foldamers contains H-bonds that differ in terms of favorability, with the  $\gamma$  residue  $C=O(i) \rightarrow \alpha$  residue  $H-N(i+3)$  H-bonds intrinsically superior to the  $\alpha$  residue  $C=O(i) \rightarrow \gamma$  residue  $H-N(i-1)$  H-bonds. This possibility was initially suggested by the seven crystal structures described here, in which the  $\alpha$  residue  $C=O(i) \rightarrow \gamma$  residue  $H-N(i-1)$  H-bond distances were long or other molecules were interpolated into these interactions. Such interpolations have occasionally been observed in proteins<sup>21</sup> or short conventional peptides<sup>22</sup> and more recently in  $\alpha/\gamma$ -peptides,<sup>23</sup> but the frequency of this unusual phenomenon in our structural data set stands out. HDX and DMSO titration results support the conclusion that there is an energetic differentiation between the two types of H-bond in the 12/10-helical conformation formed by the  $\alpha/\gamma(I)$  backbone. We speculate that the  $\gamma(I)$  residue is not ideally preorganized for the 10-atom H-bonding mode.<sup>17</sup> Several foldamer secondary

Table 1. Relative HDX Half-Life Data for Octamer 5, Normalized to Dimer 6.



	Phe-1	$\gamma$ (I)-2	Phe-3	$\gamma$ (I)-4	Phe-5	$\gamma$ (I)-6	Phe-7	$\gamma$ (I)-8
$t_{1/2}$ (h)	2.2	102	95	199	121	— <sup>a</sup>	46	37
normalized $t_{1/2}$	1.7	13	73	25	93	— <sup>a</sup>	35	4.6
H-bonded ring size	—	10	12	10	12	10	12	—

<sup>a</sup>Resonance overlapped with phenyl H.

structures containing different H-bond types have been discovered, and our results raise the possibility that topologically distinct H-bonds will in general be energetically differentiated.

## ■ ASSOCIATED CONTENT

### ■ Supporting Information

Synthetic routes, NMR data, details of NMR structure calculations for 4 and other foldamers, DMSO titration data, HDX data, helix and H-bond parameters for crystal structures, crystallographic data, and zip files containing CIF and PDB files. The Supporting Information is available free of charge on the ACS Publications website at DOI: 10.1021/jacs.5b03382.

## ■ AUTHOR INFORMATION

### ■ Corresponding Author

\*gellman@chem.wisc.edu

### ■ Present Address

†L.G.: Halliburton, 3000 N Sam Houston Parkway E, Houston, TX 77032, United States.

### ■ Notes

The authors declare no competing financial interest.

## ■ ACKNOWLEDGMENTS

This work was supported by NSF Grant CHE-1307365. NMR spectrometers used in this work were purchased with support from a generous gift by Paul J. Bender and from NIH (1 S10 RR13866-01). The authors thank Dr. Michael W. Giuliano for helpful discussions regarding CNS calculations, Dr. Young-Hee Shin for assistance in acquiring 2D NMR spectra, and Dr. Matt Benning for acquiring single-crystal diffraction data of 2b at the Bruker AXS facility in Fitchburg, WI.

## ■ REFERENCES

- (1) (a) Gellman, S. H. *Acc. Chem. Res.* **1998**, *31*, 173. (b) Hill, D. J.; Mio, M. J.; Prince, R. B.; Hughes, T. S.; Moore, J. S. *Chem. Rev.* **2001**, *101*, 3893. (c) Guichard, G.; Huc, I. *Chem. Commun.* **2011**, *47*, 5933.
- (2) (a) Cheng, R. P.; Gellman, S. H.; DeGrado, W. F. *Chem. Rev.* **2001**, *101*, 3219. (b) Seebach, D.; Hook, D. F.; Glättli, A. *Biopolymers* **2006**, *84*, 23.
- (3) Reinert, Z. E.; Horne, W. S. *Org. Biomol. Chem.* **2014**, *12*, 8796.
- (4) (a) Hamuro, Y.; Schneider, J. P.; DeGrado, W. F. *J. Am. Chem. Soc.* **1999**, *121*, 12200. (b) Porter, E. A.; Wang, X.; Lee, H. S.; Weisblum, B.; Gellman, S. H. *Nature* **2000**, *404*, 565. (c) Stephens, O. M.; Kim, S.; Welch, B. D.; Hodsdon, M. E.; Kay, M. S.; Schepartz, A. *J. Am. Chem. Soc.* **2005**, *127*, 13126. (d) English, E. P.; Chumanov, R. S.; Gellman, S. H.; Compton, T. *J. Biol. Chem.* **2006**, *281*, 2661. (e) Gademann, K.; Kimmerlin, T.; Hoyer, D.; Seebach, D. *J. Med. Chem.* **2001**, *44*, 2460. (f) Seebach, D.; Schaeffer, L.; Brenner, M.; Hoyer, D. *Angew. Chem., Int. Ed.* **2003**, *42*, 776.
- (5) (a) Horne, W. S.; Gellman, S. H. *Acc. Chem. Res.* **2008**, *41*, 1399. (b) Pendem, N.; Nelli, Y. R.; Douat, C.; Fischer, L.; Laguerre, M.; Ennifar, E.; Kauffmann, B.; Guichard, G. *Angew. Chem., Int. Ed.* **2013**, *52*,

4147. (c) Wu, H.; Qiao, Q.; Hu, Y.; Teng, P.; Gao, W.; Zuo, X.; Wojtas, L.; Larsen, R. W.; Ma, S.; Cai, J. *Chem.—Eur. J.* **2015**, *21*, 2501.

(6) (a) Sadowsky, J. D.; Schmitt, M. A.; Lee, H. S.; Umezawa, N.; Wang, S.; Tomita, Y.; Gellman, S. H. *J. Am. Chem. Soc.* **2005**, *127*, 11966. (b) Sadowsky, J. D.; Fairlie, W. D.; Hadley, E. B.; Lee, H. S.; Umezawa, N.; Nikolovska-Coleska, Z.; Wang, S.; Huang, D. C.; Tomita, Y.; Gellman, S. H. *J. Am. Chem. Soc.* **2007**, *129*, 139. (c) Johnson, L. M.; Gellman, S. H. *Methods Enzymol.* **2013**, *523*, 407.

(7) Seebach, D.; Gademann, K.; Schreiber, J. V.; Matthews, J. L.; Hintermann, T.; Jaun, B.; Oberer, L.; Hommel, U.; Widmer, H. *Helv. Chim. Acta* **1997**, *80*, 2033.

(8) Szolnoki, É.; Hetényi, A.; Mándity, I. M.; Fülöp, F.; Martinek, T. A. *Eur. J. Org. Chem.* **2013**, 3555.

(9) Sharma, G. V.; Nagendar, P.; Jayaprakash, P.; Radha Krishna, P.; Ramakrishna, K. V.; Kunwar, A. C. *Angew. Chem., Int. Ed.* **2005**, *44*, 5878.

(10) (a) Berlicki, L.; Pils, L.; Wéber, E.; Mándity, I. M.; Cabrele, C.; Martinek, T. A.; Fülöp, F.; Reiser, O. *Angew. Chem., Int. Ed.* **2012**, *51*, 2208. (b) Legrand, B.; André, C.; Moulat, L.; Wenger, E.; Didierjean, C.; Aubert, E.; Averlant-Petit, M. C.; Martinez, J.; Calmes, M.; Amblard, M. *Angew. Chem., Int. Ed.* **2014**, *53*, 13131.

(11) Guo, L.; Chi, Y.; Almeida, A. M.; Guzei, I. A.; Parker, B. K.; Gellman, S. H. *J. Am. Chem. Soc.* **2009**, *131*, 16018.

(12) Guo, L.; Zhang, W.; Reidenbach, A. G.; Giuliano, M. W.; Guzei, I. A.; Spencer, L. C.; Gellman, S. H. *Angew. Chem., Int. Ed.* **2011**, *50*, 5843.

(13) Guo, L.; Almeida, A. M.; Zhang, W.; Reidenbach, A. G.; Choi, S. H.; Guzei, I. A.; Gellman, S. H. *J. Am. Chem. Soc.* **2010**, *132*, 7868.

(14) Mándity, I. M.; Weber, E.; Martinek, T. A.; Olajos, G.; Tóth, G. K.; Vass, E.; Fülöp, F. *Angew. Chem., Int. Ed.* **2009**, *48*, 2171.

(15) Crystallographic data have been deposited at the Cambridge Crystallographic Data Centre with accession codes 1056028–1056034 and can be accessed free of charge at [www.ccdc.cam.ac.uk/data\\_request/cif](http://www.ccdc.cam.ac.uk/data_request/cif).

(16) (a) Yeates, T. O.; Kent, S. B. *Annu. Rev. Biophys.* **2012**, *41*, 41. (b) Lee, M.; Shim, J.; Kang, P.; Guzei, I. A.; Choi, S. H. *Angew. Chem., Int. Ed.* **2013**, *52*, 12564.

(17) See the Supporting Information.

(18) Jeffrey, G. A. *An Introduction to Hydrogen Bonding*; Oxford University Press: New York, 1997.

(19) (a) Sharma, G. V.; Jadhav, V. B.; Ramakrishna, K. V.; Jayaprakash, P.; Narsimulu, K.; Subash, V.; Kunwar, A. C. *J. Am. Chem. Soc.* **2006**, *128*, 14657. (b) Giuliano, M. W.; Maynard, S. J.; Almeida, A. M.; Guo, L.; Guzei, I. A.; Spencer, L. C.; Gellman, S. H. *J. Am. Chem. Soc.* **2014**, *136*, 15046.

(20) Bai, Y.; Milne, J. S.; Mayne, L.; Englander, S. W. *Proteins* **1993**, *17*, 75.

(21) Sundaralingam, M.; Sekharudu, Y. C. *Science* **1989**, *244*, 1333.

(22) Karle, I. L.; Flippin-Anderson, J.; Uma, K.; Balaram, P. *Proc. Natl. Acad. Sci. U.S.A.* **1988**, *85*, 299.

(23) (a) Basuroy, K.; Dinesh, B.; Shamala, N.; Balaram, P. *Angew. Chem.* **2013**, *125*, 3218. (b) Basuroy, K.; Dinesh, B.; Shamala, N.; Balaram, P. *Angew. Chem., Int. Ed.* **2013**, *52*, 3136. (c) Karle, I. L.; Flippin-Anderson, J. L.; Uma, K.; Balaram, P. *Int. J. Pept. Protein Res.* **1994**, *44*, 491.